Chapter 9

Method of Lines

"Prejudice is the child of ignorance." William Hazlitt

9.1 Introduction

The method of lines (MOL) is a well-established numerical technique (or rather a semianalytical method) for the analysis of transmission lines, waveguide structures, and scattering problems. The method was originally developed by mathematicians and used for boundary value problems in physics and mathematics (e.g., [1]–[5]). A review of these earlier uses (1930–1965) of MOL is found in Liskovets [6]. The method was introduced into the EM community around 1980 and further developed by Pregla et al. [7]–[14] and other researchers. Although the formulation of this modern application is different from the earlier approach, the basic principles are the same.

The method of lines is regarded as a special finite difference method but more effective with respect to accuracy and computational time than the regular finite difference method. It basically involves discretizing a given differential equation in one or two dimensions while using analytical solution in the remaining direction. MOL has the merits of both the finite difference method and analytical method; it does not yield spurious modes nor does it have the problem of "relative convergence."

Besides, the method of lines has the following properties that justify its use:

(a) Computational efficiency: the semianalytical character of the formulation leads to a simple and compact algorithm, which yields accurate results with less computational effort than other techniques.

(b) Numerical stability: by separating discretization of space and time, it is easy to establish stability and convergence for a wide range of problems.

(c) Reduced programming effort: by making use of the state-of-the-art well documented and reliable ordinary differential equations (ODE) solvers, programming effort can be substantially reduced.

© 2001 by CRC PRESS LLC

(d) Reduced computational time: since only a small amount of discretization lines are necessary in the computation, there is no need to solve a large system of equations; hence computing time is small.

To apply MOL usually involves the following five basic steps:

- partitioning the solution region into layers
- discretization of the differential equation in one coordinate direction
- transformation to obtain decouple ordinary differential equations
- inverse transformation and introduction of the boundary conditions
- solution of the equations

We begin to apply these steps to the problem of solving Laplace's equation. Since MOL involves many matrix manipulations, it is expedient that all computer codes in chapters are written in Matlab.

9.2 Solution of Laplace's Equation

Although the method of lines is commonly used in the EM community for solving hyperbolic (wave equation), it can be used to solve parabolic and elliptic equations [1], [15]–[18]. In this section, we consider the application of MOL to solve Laplace's equation (elliptic problem) involving two-dimensional rectangular and cylindrical regions.

9.2.1 Rectangular Coordinates

Laplace's equation in Cartesian system is

$$\frac{\partial^2 V}{\partial x^2} + \frac{\partial^2 V}{\partial y^2} = 0 \tag{9.1}$$

Consider a two-dimensional solution shown in Fig. 9.1. The first step is discretization of the x-variable. The region is divided into strips by N dividing straight lines (hence the name *method of lines*) parallel to the y-axis. Since we are discretizing along x, we replace the second derivative with respect to x with its finite difference equivalent. We apply the three-point central difference scheme,

$$\frac{\partial^2 V_i}{\partial x^2} = \frac{V_{i+1} - 2V_i + V_{i-1}}{h^2} \tag{9.2}$$

© 2001 by CRC PRESS LLC

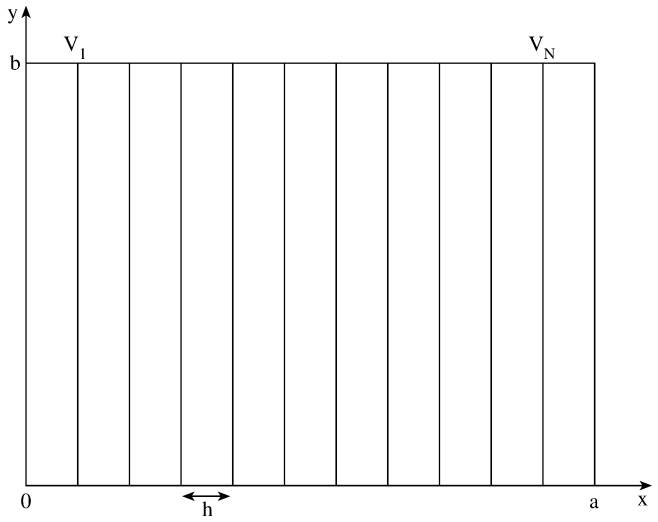

Figure 9.1
Illustration of discretization in the x-direction.

where h is the spacing between discretized lines, i.e.,

$$h = \Delta x = \frac{a}{N+1} \tag{9.3}$$

Replacing the derivative with respect to x by its finite difference equivalent, Eq. (9.1) becomes

$$\frac{\partial^2 V_i}{\partial y^2} + \frac{1}{h^2}\left[V_{i+1}(y) - 2V_i(y) + V_{i-1}(y)\right] = 0 \tag{9.4}$$

Thus the potential V in Eq. (9.1) can be replaced by a vector of size N, namely

$$[V] = [V_1, V_2, \ldots, V_N]^t \tag{9.5a}$$

where t denotes the transpose,

$$V_i(y) = V(x_i, y), \;\; i = 1.2, \ldots, N \tag{9.5b}$$

and $x_i = i\,\Delta x$. Substituting Eqs. (9.4) and (9.5) into Eq. (9.1) yields

$$\frac{\partial^2 [V(y)]}{\partial y^2} - \frac{1}{h^2}[P][V(y)] = [0] \tag{9.6}$$

© 2001 by CRC PRESS LLC

where [0] is a zero column vector and $[P]$ is an $N \times N$ tridiagonal matrix representing the discretized form of the second derivative with respect to x.

$$[P] = \begin{bmatrix} p_\ell & -1 & 0 & \dots & 0 \\ -1 & 2 & -1 & \dots & 0 \\ & \ddots & \ddots & \ddots & \\ 0 & \dots & -1 & 2 & -1 \\ 0 & \dots & 0 & -1 & p_r \end{bmatrix} \tag{9.7}$$

All the elements of matrix $[P]$ are zeros except the tridiagonal terms; the elements of the first and the last row of $[P]$ depend on the boundary conditions at $x = 0$ and $x = a$. $p_\ell = 2$ for Dirichlet boundary condition and $p_\ell = 1$ for Neumann boundary condition. The same is true of p_r.

The next step is to analytically solve the resulting equations along the y coordinate. To solve Eq. (9.6) analytically, we need to obtain a system of uncoupled ordinary differential equations from the coupled equations (9.6). To achieve this, we define the transformed potential $[\overline{V}]$ by letting

$$\big[V\big] = \big[T\big]\big[\overline{V}\big] \tag{9.8}$$

and requiring that

$$\big[T\big]^t\big[P\big]\big[T\big] = \big[\lambda^2\big] \tag{9.9}$$

where $[\lambda^2]$ is a diagonal matrix and $[T]^t$ is the transpose of $[T]$. $[\lambda^2]$ and $[T]$ are eigenvalue and eigenvector matrices belonging to $[P]$. The transformation matrix $[T]$ and the eigenvalue matrix $[\lambda^2]$ depend on the boundary conditions and are given in Table 9.1 for various combinations of boundaries. It should be noted that the

Table 9.1 Elements of Transformation Matrix $[T]$ and Eigenvalues

Left boundary	Right boundary	T_{ij}	λ_i
Dirichlet	Dirichlet	$\sqrt{\frac{2}{N+1}} \sin \frac{ij\pi}{N+1}$, $[T_{DD}]$	$2 \sin \frac{i\pi}{2(N+1)}$
Dirichlet	Neumann	$\sqrt{\frac{2}{N+0.5}} \sin \frac{i(j-0.5)\pi}{N+0.5}$, $[T_{DN}]$	$2 \sin \frac{(i-0.5)\pi}{2N+1}$
Neumann	Dirichlet	$\sqrt{\frac{2}{N+0.5}} \cos \frac{(i-0.5)(j-0.5)\pi}{N+0.5}$, $[T_{ND}]$	$2 \sin \frac{(i-0.5)\pi}{2N+1}$
Neumann	Neumann	$\sqrt{\frac{2}{N}} \cos \frac{(i-0.5)(j-1)\pi}{N}$, $j > 1$, $[T_{NN}]$	$2 \sin \frac{(i-1)\pi}{2N}$
		$\frac{1}{\sqrt{N}}$, $j = 1$	

Note: where $i, j = 1, 2, \dots, N$ and subscripts D and N are for Dirichlet and Neumann conditions, respectively.

© 2001 by CRC PRESS LLC

eigenvector matrix $[T]$ has the following properties:

$$[T]^{-1} = [T]^t$$
$$[T][T]^t = [T]^t[T] = [I] \tag{9.10}$$

where $[I]$ is an identity matrix. Substituting Eq. (9.8) into Eq. (9.6) gives

$$\frac{\partial^2[T][\overline{V}]}{\partial y^2} - \frac{1}{h^2}[P][T][\overline{V}] = [0]$$

Multiplying through by $[T]^{-1} = [T]^t$ yields

$$\left(\frac{\partial^2}{\partial y^2} - \frac{1}{h^2}[\lambda^2]\right)[\overline{V}] = [0] \tag{9.11}$$

This is an ordinary differential equation with solution

$$\overline{V}_i = A_i \cosh \alpha_i y + B_i \sinh \alpha_i y \tag{9.12}$$

where $\alpha_i = \lambda_i / h$.

Thus, Laplace's equation is solved numerically using a finite difference scheme in the x-direction and analytically in the y-direction. However, we have only demonstrated three out of the five basic steps for applying MOL. There remain two more steps to complete the solution: imposing the boundary conditions and solving the resulting equations. Imposing the boundary conditions is problem dependent and will be illustrated in Example 9.1. The resulting equations can be solved using the existing packages for solving ODE or developing our own codes in Fortran, Matlab, C, or any programming language. We will take the latter approach in Example 9.1.

Example 9.1

For the rectangular region in Fig. 9.1, let

$$V(0, y) = V(a, y) = V(x, 0) = 0\,, \quad V(x, b) = 100$$

and $a = b = 1$. Find the potential at (0.25, 0.75), (0.5, 0.5), (0.75, 0.25). □

Solution

In this case, we have Dirichlet boundaries at $x = 0$ and $x = 1$, which are already indirectly taken care of in the solution in Eq. (9.12). Hence, from Table 9.1,

$$\lambda_i = 2 \sin \frac{i\pi}{2(N+1)} \tag{9.13}$$

and

$$T_{ij} = \sqrt{\frac{2}{N+1}} \sin \frac{ij\pi}{N+1} \tag{9.14}$$

© 2001 by CRC PRESS LLC

Let $N = 15$ so that $h = \Delta x = 1/16$ and $x = 0.25, 0.5, 0.75$ will correspond to $i = 4, 8, 12$, respectively.

By combining Eqs. (9.8) and (9.12), we obtain the required solution. To get constants A_i and B_i, we apply boundary conditions at $y = 0$ and $y = b$ to V and perform inverse transformation. Imposing $V(x, y = 0) = 0$ to the combination of Eqs. (9.8) and (9.12), we obtain

$$\begin{bmatrix} V_1 \\ V_2 \\ \vdots \\ V_N \end{bmatrix} = [0] = \begin{bmatrix} T_{11} & T_{12} & \dots & T_{1N} \\ T_{21} & T_{22} & \dots & T_{2N} \\ \vdots & & \dots & \vdots \\ T_{N1} & T_{N2} & \dots & T_{NN} \end{bmatrix} \begin{bmatrix} A_1 \\ A_2 \\ \vdots \\ A_N \end{bmatrix}$$

which implies that

$$[A] = 0 \quad \text{or} \quad A_i = 0 \tag{9.15}$$

Imposing $V(x, y = b) = 100$ yields

$$\begin{bmatrix} 100 \\ 100 \\ \vdots \\ 100 \end{bmatrix} = [T] \begin{bmatrix} B_1 \sinh \alpha_1 b \\ B_2 \sinh \alpha_2 b \\ \vdots \\ B_N \sinh \alpha_N b \end{bmatrix}$$

If we let

$$[C] = \begin{bmatrix} B_1 \sinh \alpha_1 b \\ B_2 \sinh \alpha_2 b \\ \vdots \\ B_N \sinh \alpha_N b \end{bmatrix} = [T]^{-1} \begin{bmatrix} 100 \\ 100 \\ \vdots \\ 100 \end{bmatrix}$$

then

$$B_i = C_i / \sinh \alpha_i b \tag{9.16}$$

With A_i and B_i found in Eqs. (9.15) and (9.16), the potential $V(x, y)$ is determined as

$$V_i(y) = \sum_{j=1}^{N} T_{ij} B_j \sinh(\alpha_j y) \tag{9.17}$$

By applying Eqs. (9.13) to (9.17), the Matlab code in Fig. 9.2 was developed to obtain

$$V(0.25, 0.75) = 43.1\,, \quad V(0.5, 0.5) = 24.96\,, \quad V(0.75, 0.25) = 6.798$$

The result compares well with the exact solution:

$$V(0.25, 0.75) = 43.2\,, \quad V(0.5, 0.5) = 25.0\,, \quad V(0.75, 0.25) = 6.797$$

© 2001 by CRC PRESS LLC

```
AA = 1;
BB = 1;
N = 15;
% DETERMINE VECTOR ALPHA
H = AA/(N+1);
LAM = 2*sin ((1:N)*pi*0.5/(N+1) );
ALPHA = LAM/H;
% CALCULATE THE TRANSFORMATION MATRIX AND COEFFICIENT B
K = sqrt (2/(N+1));
T = zeros(N,N);
for  I=1:N
  for J=1:N
    T(I,J) = K*sin (I*J*pi/(N+1));
  end
end
V = 100*ones(N,1);
C = inv(T)*V;
A = ALPHA';
B = C./sinh(BB*A);
% CALCULATE V AT THE GIVEN POINTS
V1 = 0;  V2 = 0;  V3 = 0;
for K=1:N
V1 = V1 + T(4,K)*B(K)*sinh(ALPHA(K)*0.75);
V2 = V2 + T(8,K)*B(K)*sinh(ALPHA(K)*0.5);
V3 = V3 + T(12,K)*B(K)*sinh(ALPHA(K)*0.25);
end
diary
V1, V2, V3
diary off
```

Figure 9.2
Matlab code for Example 9.1.

Notice that it is not necessary to invert the transformation matrix $[T]$ in view of Eq. (9.10). ∎

Example 9.2

For Dirichlet–Neumann conditions, derive the transformation matrix $[T_{DN}]$ and the corresponding eigenvalues $[\lambda^2]$. □

Solution

Let λ_k^2 be the elements of eigenvalue matrix $[\lambda^2]$ and $[t_k]$ be the column vectors of the transformation matrix $[T_{DN}]$ corresponding to matrix $[P]$. Then, by definition,

$$\left([P] - \lambda_k^2[I]\right)[t_k] = [0] \tag{9.18}$$

Substituting $[P]$ for Dirichlet–Neumann condition in Eq. (9.7) into Eq. (9.18) gives

© 2001 by CRC PRESS LLC

a second-order difference equation

$$-t_{i-1}^{(k)} + \left(2 - \lambda_k^2\right) t_i^{(k)} - t_{i+1}^{(k)} = 0 \tag{9.19}$$

except the first and last equations in (9.18). If we let

$$t_i^{(k)} = A_k e^{ji\phi_k} + B_k e^{-ji\phi_k} \tag{9.20}$$

and substitute this into Eq. (9.19), we obtain

$$0 = \left(A_k e^{ji\phi_k} + B_k e^{-ji\phi_k}\right)\left(-2\cos\phi_k + 2 - \lambda_k^2\right)$$

from which we obtain the characteristic equation

$$\lambda_k^2 = 2\left(1 - \cos\phi_k\right) = 4\sin^2\frac{\phi_k}{2} \tag{9.21}$$

or

$$\lambda_k = 2\sin\frac{\phi_k}{2} \tag{9.22}$$

This is valid for all types of boundary combinations but ϕ_k will depend on the boundary conditions. To determine ϕ_k, A_k, and B_k, we use the first and the last equations in Eq. (9.18). For DN conditions,

$$t_0^{(k)} = 0 \tag{9.23a}$$

$$-t_N^{(k)} + t_{N+1}^{(k)} = 0 \tag{9.23b}$$

Substituting this into Eq. (9.20), we obtain

$$\begin{bmatrix} 1 & 1 \\ e^{jN\phi_k}\left(e^{j\phi_k} - 1\right) & e^{-jN\phi_k}\left(e^{-j\phi_k} - 1\right) \end{bmatrix} \begin{bmatrix} A_k \\ B_k \end{bmatrix} = \begin{bmatrix} 0 \end{bmatrix} \tag{9.24}$$

For nontrivial solutions,

$$\phi_k = \frac{k - 0.5}{N + 0.5}\pi\ , \quad k = 1, 2, \ldots, N \tag{9.25}$$

Also from Eqs. (9.23a) and (9.20), $A_k = -B_k$ so that

$$t_i^{(k)} = A_k \sin\left(i\phi_k\right) \tag{9.26}$$

Thus, for Dirichlet–Neumann conditions, we obtain

$$\lambda_k = 2\sin\left(0.5\pi\frac{k - 0.5}{N + 0.5}\right) \tag{9.27a}$$

$$T_{ij} = \sqrt{\frac{2}{N + 0.5}}\sin\left(0.5\pi\frac{i(k - 0.5)}{N + 0.5}\right) \tag{9.27b}$$

© 2001 by CRC PRESS LLC

9.2.2 Cylindrical Coordinates

Although MOL is not applicable to problems with complex geometry, the method can be used to analyze homogeneous and inhomogeneous cylindrical problems. The principal steps in applying MOL in cylindrical coordinates are the same as in Cartesian coordinates.

Here, we illustrate with the use of MOL to solve Laplace's equation in cylindrical coordinates [18]. We apply discretization procedure in the angular direction. The resulting coupled ordinary differential equations are decoupled by matrix transformation and solved analytically.

Assume that we are interested in finding the potential distribution in a cylindrical transmission line with a uniform but arbitrary cross section. We assume that the inner conductor is grounded while the outer conductor is maintained at constant potential V_o, as shown in Fig. 9.3. In cylindrical coordinates (ρ, ϕ), Laplace's equation can be

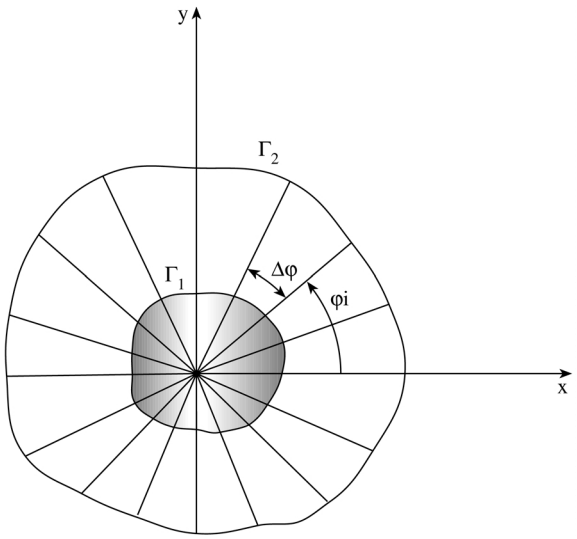

Figure 9.3
Discretization along φ-direction.

expressed as

$$\rho^2 \frac{\partial^2 V}{\partial \rho^2} + \rho^2 \frac{\partial V}{\partial \rho} + \frac{\partial^2 V}{\partial \phi^2} = 0 \tag{9.28}$$

subject to

$$V(\rho) = 0\,, \quad \rho \in \Gamma_1 \tag{9.29a}$$
$$V(\rho) = V_o\,, \quad \rho \in \Gamma_2 \tag{9.29b}$$

© 2001 by CRC PRESS LLC

We discretize in the ϕ-direction by using N radial lines, as shown in Fig. 9.3, such that

$$V_i(\rho) = V(\rho, \phi_i) , \quad i = 1.2, \ldots, N \tag{9.30}$$

where

$$\phi_i = ih = \frac{2\pi i}{N} , \; h = \Delta\phi = \frac{2\pi}{N} \tag{9.31}$$

and h is the angular spacing between the lines. We have subdivided the solution region into N subregions with boundaries at Γ_1 and Γ_2. In each subregion, $V(\rho, \phi)$ is approximated by $V_i = V(\rho, \phi_i)$, with ϕ_i being constant.

Applying the three-point central finite difference scheme yields

$$\frac{\partial^2[V]}{\partial\phi^2} = -\frac{[P]}{h^2}[V] \tag{9.32}$$

where

$$[V] = [V_1, V_2, \ldots, V_N]^t \tag{9.33}$$

and

$$[P] = \begin{bmatrix} 2 & -1 & 0 & 0 & \ldots & 0 & 0 & -1 \\ -1 & 2 & -1 & 0 & \ldots & 0 & 0 & 0 \\ 0 & -1 & 2 & -1 & \ldots & 0 & 0 & 0 \\ \vdots & \vdots & \vdots & \vdots & \ldots & \vdots & \vdots & \vdots \\ 0 & 0 & 0 & 0 & \ldots & -1 & 2 & -1 \\ -1 & 0 & 0 & 0 & \ldots & 0 & -1 & 2 \end{bmatrix} \tag{9.34}$$

Notice that $[P]$ contains an element -1 in the lower left and upper right corners due to its angular periodicity. Also, notice that $[P]$ is a quasi-three-band symmetric matrix which is independent of the arbitrariness of the cross section as a result of the discretization over a finite interval $[0, 2\pi]$.

Introducing Eq. (9.32) into Eq. (9.28) leads to the following set of coupled differential equations

$$\rho^2\frac{\partial^2[V]}{\partial\rho^2} + \rho\frac{\partial[V]}{\partial\rho} - \frac{[P]}{h^2}[V] = 0 \tag{9.35}$$

To decouple Eq. (9.35), we must diagonalize $[P]$ by an orthogonal matrix $[T]$ such that

$$\left[\lambda^2\right] = \left[T\right]^t\left[P\right]\left[T\right] \tag{9.36}$$

with

$$[T]^t = [T] = [T]^{-1} \tag{9.37}$$

© 2001 by CRC PRESS LLC

where $[\lambda^2]$ is a diagonal matrix of the eigenvalues λ_n^2 of $[P]$. The diagonalization is achieved using [19]

$$T_{ij} = \frac{\cos\alpha_{ij} + \sin\alpha_{ij}}{\sqrt{N}}\ , \quad \lambda_n^2 = 2(1 - \cos\alpha_n) \tag{9.38}$$

where

$$\alpha_{ij} = h \cdot i \cdot j\ , \quad \alpha_n = h \cdot n\ , \quad i, j, n = 1, 2, \ldots, N \tag{9.39}$$

If we introduce the transformed potential U that satisfies

$$[U] = [T][V] \tag{9.40}$$

Equation (9.35) becomes

$$\rho^2 \frac{\partial^2[U]}{\partial\rho^2} + \rho\frac{\partial[U]}{\partial\rho} - \Big[\mu^2\Big]\Big[U\Big] = 0 \tag{9.41}$$

where

$$\Big[U\Big] = \Big[U_1, U_2, \ldots, U_N\Big]^t \tag{9.42}$$

is a vector containing the transformed potential function and

$$\mu_n = \frac{\lambda_n}{h} = \frac{2}{h}\sin(\alpha_n/2) \tag{9.43}$$

Equation (9.41) is the Euler-type and has the analytical solution (see Section 2.4.1)

$$U_n = \begin{cases} A_n + B_n \ln\rho\ , & \mu_n = 0 \\ A_n\rho^{\mu_n} + B_n\rho^{-\mu_n}\ , & \mu_n \neq 0 \end{cases} \tag{9.44}$$

This is applied to each subregion. By taking the inverse transform using Eq. (9.40), we obtain the potential $V_i(\rho)$ as

$$V_i(\rho) = \sum_{j=1}^{N} T_{ij}U_j \tag{9.45}$$

where T_{ij} are the elements of matrix $[T]$.

We now impose the boundary conditions in Eq. (9.29), which can be rewritten as

$$V(\rho = r_i) = 0\ , \quad r_i \in \Gamma_1 \tag{9.46a}$$

$$V(\rho = R_i) = V_o\ , \quad R_i \in \Gamma_2 \tag{9.46b}$$

© 2001 by CRC PRESS LLC

Applying these to Eqs. (9.44) and (9.45),

$$T_{ij}\left[A_j + B_j \ln r_i\right]\Big|_{\mu_j=0} + \sum_{j=1}^{N} T_{ij}\left[A_j r_i^{\mu_j} + B_j r_i^{-\mu_j}\right]\Big|_{\mu_j\neq 0} = 0\ ,$$
$$i = 1, 2, \ldots, N \tag{9.47a}$$

$$T_{ij}\left[A_j + B_j \ln R_i\right]\Big|_{\mu_j=0} + \sum_{j=1}^{N} T_{ij}\left[A_j R_i^{\mu_j} + B_j R_i^{-\mu_j}\right]\Big|_{\mu_j\neq 0} = V_o\ ,$$
$$i = 1, 2, \ldots, N \tag{9.47b}$$

Equation (9.47) is solved to determine the unknown coefficients A_i and B_i. The potential distribution is finally obtained from Eqs. (9.44) and (9.45).

Example 9.3

Consider a coaxial cable with inner radius a and outer radius b. Let $b = 2a = 2$ cm and $V_o = 100$ V. This simple example is selected to be able to compare MOL solution with the exact solution □

Solution

From Eq. (9.43), it is evident that $\mu_n = 0$ only when $n = N$. Hence, we may write U as

$$U_n = \begin{cases} A_n \rho^{\mu_n} + B_n \rho^{-\mu_n}\ , & n = 1, 2, \ldots, N-1 \\ A_n + B_n \ln \rho\ , & n = N \end{cases} \tag{9.48}$$

Equation (9.47) can be written as

$$\sum_{j=1}^{N-1} T_{ij}\left[A_j a_i^{\mu_j} + B_j a_i^{-\mu_j}\right] + T_{iN}\left[A_N + B_N \ln a\right] = 0\ ,$$
$$i = 1, 2, \ldots, N \tag{9.49a}$$

for $\rho = a$, and

$$\sum_{j=1}^{N-1} T_{ij}\left[A_j b_i^{\mu_j} + B_j b_i^{-\mu_j}\right] + T_{iN}\left[A_N + B_N \ln b\right] = V_o\ ,$$
$$i = 1, 2, \ldots, N \tag{9.49b}$$

for $\rho = b$. These $2N$ equations will enable us to find the $2N$ unknown coefficients

© 2001 by CRC PRESS LLC

A_i and B_i. They can be cast into a matrix form as

$$\begin{bmatrix} T_{11}A_1a^{\mu_1} & \dots & T_{1N}A_N & T_{11}B_1a^{-\mu_1} & \dots & B_N \ln a \\ \vdots & & & & & \vdots \\ T_{N1}A_1a^{\mu_1} & \dots & T_{NN}A_N & T_{N1}B_1a^{-\mu_1} & \dots & B_N \ln a \\ T_{11}A_1b^{\mu_1} & \dots & T_{1N}A_N & T_{11}B_1b^{-\mu_1} & \dots & B_N \ln b \\ \vdots & & & & & \vdots \\ T_{N1}A_1b^{\mu_1} & \dots & T_{NN}A_N & T_{N1}B_1b^{-\mu_1} & \dots & B_N \ln b \end{bmatrix} \begin{bmatrix} A_1 \\ A_2 \\ \vdots \\ A_N \\ B_1 \\ B_2 \\ \vdots \\ B_N \end{bmatrix} = \begin{bmatrix} 0 \\ 0 \\ \vdots \\ 0 \\ 100 \\ 100 \\ \vdots \\ 100 \end{bmatrix} \tag{9.50}$$

This can be written as

$$[D][C] = [F] \tag{9.51}$$

from which we obtain

$$[C] = [D]^{-1}[F] \tag{9.52}$$

where C_j corresponds to A_j when $j = 1, 2, \dots, N$ and C_j corresponds to B_j when $j = N + 1, \dots, 2N$.

Once A_j and B_j are known, we substitute them into Eq. (9.48) to find U_j. We finally apply Eq. (9.45) to find V. The exact analytical solution of the problem is

$$V(\rho) = V_o \frac{\ln \frac{\rho}{a}}{\ln \frac{b}{a}} \tag{9.53}$$

For $a < \rho < b$, we obtain V for both exact and MOL solutions using the Matlab codes in Fig. 9.4. The results of the two solutions are shown in Fig. 9.5. The two solutions agree perfectly. ∎

9.3 Solution of Wave Equation

The method of lines is particularly suitable for modeling a wide range of transmission lines and planar waveguide structures with multiple layers [8, 11, 19]–[29]. This involves discretizing the Helmholtz wave equation in one direction while the other direction is treated analytically. Here we consider the general problem of two-layer structures covered on the top and bottom with perfectly conducting planes. The conducting strips are assumed to be thin. We will illustrate with two-layer planar and cylindrical microstrip structures.

© 2001 by CRC PRESS LLC

```
EXAMPLE 9.3 SOLVED USING METHOD OF LINES

% OUR OBJECTIVE IS TO DETERMINE THE POTENTIAL
% DISTRIBUTION IN A COAXIAL CABLE OF INNER RADIUS a
% AND OUTER RADIUS b ASSUMING A POTENTIAL DIFFERENCE OF Vo

a= 0.01; b = 0.02; Vo = 100;
N = 15;
h = 2*pi/N;
K = 1/sqrt (N);
% COMPUTE THE TRANSFORMATION MATRIX T AND MIU
T = zeros(N,N);
miu = zeros(N,1);
for  I=1:N
  miu(I) = 2*sin (I*h*0.5 )/h;
   for J=1:N
      alpha = I*J*h;
      T(I,J) = K*( cos(alpha) + sin(alpha) );
  end
end
% CALCULATE THE MATRIX D IN EQ. (9.50)
D = zeros(2*N,2*N);
for i=1:2*N
    for j=1:2*N
%Do the upper part of the matrix
        if (i <= N & j < N)
            D(i,j) = T(i,j)*a^miu(j);
        end
        if (i <= N & j == N)
             D(i,j) = T(i,j);
        end
        if (i <= N & j > N & j < 2*N)
            D(i,j) = T(i,j-N)*a^(-miu(j-N));
        end
        if (i <= N & j == 2*N)
           D(i,j) = T(i,j-N)*log(a);
        end
%Now do the lower part of the matrix
        if (i > N & i <= 2*N & j < N)
            D(i,j) = T(i-N,j)*b^miu(j);
        end
        if (i > N & i <= 2*N & j == N)
             D(i,j) = T(i-N,j);
        end
        if (i > N & i <= 2*N & j > N & j < 2*N)
            D(i,j) = T(i-N,j-N)*b^(-miu(j-N));
        end
        if (i > N & i <= 2*N & j == 2*N)
           D(i,j) = T(i-N,j-N)*log(b);
        end
    end
end
```

Figure 9.4
Matlab code for Example 9.3 ***(Continued.)***

© 2001 by CRC PRESS LLC

```
% DETERMINE THE BOUNDARY POTENTIAL MATRIX
% AND THE COEFFICIENT MATRIX
F = zeros(2*N,1);
for i=1:2*N
   if i > N
      F(i) = Vo;
   end
end
C = inv(D)*F;
% WITH THE COEFFICIENTS DETERMINED,
% NOW FIND TRANSFORMED POTENTIAL U
% AND FINALLY DETERMINE THE POTENTIAL V USING EQ. (9.45)
% WE MAY SELECT ANY VALUE OF phi, say, phi = 0^o, i.e. i=1
rho = 0.01:0.001:0.02;
M = 10; % no. of divisions along rho
Vmol = zeros(M+1,1);
for k=1:M+1
   Vmol(k) = 0.0;
   for j=1:N
    if (j <N)
   U(j) = C(j)*(rho(k))^miu(j) + C(j+N)*(rho(k))^(-miu(j));
    end
   if (j == N)
      U(j) = C(j) + C(j+N)*log(rho(k));
   end
      Vmol(k) = Vmol(k) + T(10,j)*U(j);
%        Vmol(k) = Vmol(k) + T(1,j)*U(j);
   end
end
% ALSO, CALCULATE THE EXACT VALUE OF V
Vex = Vo* (log(rho/a))/log(b/a);
diary
Vmol, Vex'
diary off
hold off
plot (rho,Vmol);
title( 'Fig. 9.5  Comparison of exact and method of lines solutions.')
xlabel('rho'), ylabel('V')
hold on
plot (rho,Vex);
hold off
```

Figure 9.4
(Cont.) **Matlab code for Example 9.3.**

© 2001 by CRC PRESS LLC

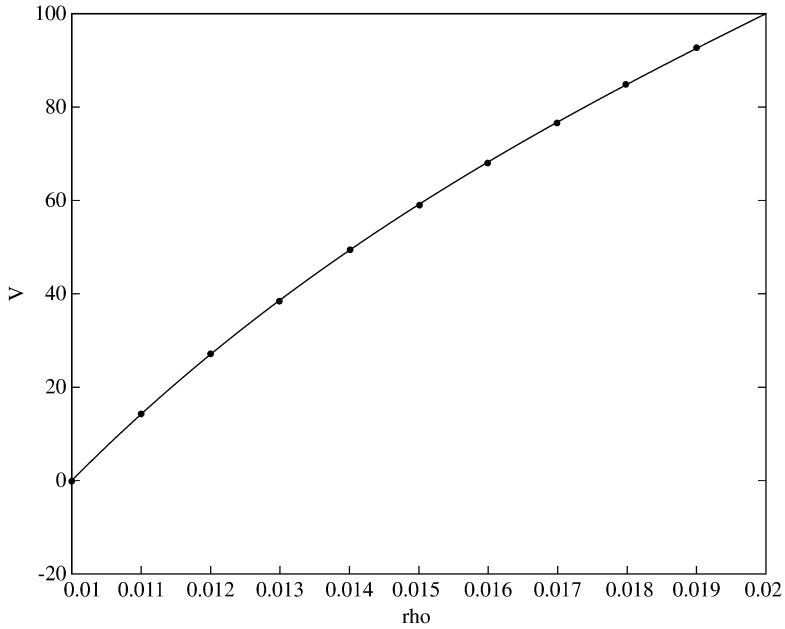

Figure 9.5
Comparison of exact and method of lines solutions.

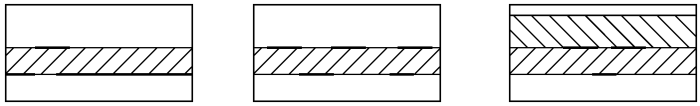

Figure 9.6
Typical planar structures.

9.3.1 Planar Microstrip Structures

Typical planar structures are shown in Fig. 9.6. The two independent field components E_z and H_z in each separate layer must satisfy the Helmholtz equation. Assuming the time factor $e^{j(\omega t-\beta z)}$ and that wave propagates along z,

$$\frac{\partial^2\psi}{\partial x}+\frac{\partial^2\psi}{\partial y}+\left(k^2-\beta^2\right)\psi=0 \tag{9.54}$$

where ψ represents either E_z or H_z and

$$k^2=\epsilon_r k_o^2\,,\quad k_o=\omega\sqrt{\mu_o\epsilon_o}=2\pi/\lambda_o \tag{9.55}$$

Applying the method of lines, we discretize the fields along the x direction by laying a family of straight lines parallel to the y axis and evaluating on the e-lines for E_z and h-lines for H_z, as shown in Fig. 9.7. The lines are evenly spaced although this is not

© 2001 by CRC PRESS LLC

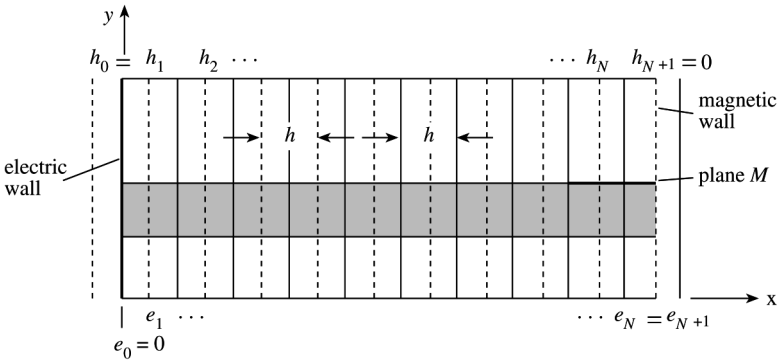

Figure 9.7
Cross section of planar microstrip structure with discretization lines; —— lines for E_z and - - - - for H_z.

necessary. If h is the spacing between adjacent lines, it is expedient to shift the e-lines and the h-lines by $h/2$ in order to guarantee a simple fitting of the literal boundary conditions. The potential in Eq. (9.54) can now be replaced by a set $[\psi_1, \psi_2, \ldots, \psi_N]$ at lines

$$x_i = x_0 + ih\ , \quad i = 1, 2, \ldots, N \tag{9.56}$$

and $\partial\psi_i/\partial x$ can be replaced by their finite difference equivalents. Thus, Eq. (9.54) becomes

$$\frac{\partial^2\psi_i}{\partial y^2} + \frac{1}{h^2}\left[\psi_{i+1}(y) - 2\psi_i(y) + \psi_{i-1}(y)\right] + k_c^2\psi_i(y) = 0\ . \qquad i = 1, 2, \ldots, N \tag{9.57}$$

where

$$k_c^2 = k^2 - \beta^2 \tag{9.58}$$

This is a system of N coupled ordinary differential equations. We cannot solve them in their present form because the equations are coupled due to the tridiagonal nature of $[P]$. We can decouple the equations by several suitable mathematical transformations and then analytically solve along the y direction.

If we let

$$\left[\psi\right] = \left[\psi_1, \psi_2, \ldots, \psi_N\right]^t \tag{9.59}$$

© 2001 by CRC PRESS LLC

where t denotes the transpose and

$$[P] = \begin{bmatrix} p_\ell & -1 & & & \\ -1 & 2 & -1 & & \\ & \ddots & \ddots & \ddots & \\ & & -1 & 2 & -1 \\ & & & -1 & p_r \end{bmatrix} \tag{9.60}$$

which is the same as Eq. (9.7) where p_ℓ and p_r are defined. Introducing the column vector $[\psi]$ and the matrix $[P]$ into Eq. (9.57) leads to

$$h^2 \frac{\partial^2 [\psi]}{\partial y^2} - \Big([P] - h^2 k_c^2 [I] \Big) [\psi] = [0] \tag{9.61}$$

where $[I]$ is the identity matrix and [0] is a zero column vector. Since $[P]$ is a real symmetric matrix, we can find an orthogonal matrix $[T]$ such that

$$\big[T\big]^t \big[P\big] \big[T\big] = \big[\lambda^2\big] \tag{9.62}$$

where the elements λ_i^2 of the diagonal matrix $[\lambda^2]$ are the eigenvalues of $[P]$. With the orthogonal matrix $[T]$, we now introduce a transformed vector $[U]$ such that

$$[T]^t [\psi] = [U] \tag{9.63}$$

We can rewrite Eq. (9.61) in terms of $[U]$ and obtain

$$h^2 \frac{\partial^2 U_i}{\partial y^2} - \Big(\lambda_i^2 - h^2 k_c^2 \Big) U_i = 0 \,, \quad i = 1, 2, \ldots, N \tag{9.64}$$

Since Eq. (9.64) is uncoupled, it can be solved analytically for each homogeneous region. The solution is similar in form to the telegraph equation. It may be expressed as a relation between U_i and its normal derivative in a homogeneous dielectric layer from $y = y_1$ to $y = y_2$, i.e.,

$$\begin{bmatrix} U_i(y_1) \\ h \frac{\partial U_i(y_1)}{dy} \end{bmatrix} = \begin{bmatrix} \cosh \alpha_i (y_1 - y_2) & \frac{1}{k_i} \sinh \alpha_i (y_1 - y_2) \\ k_i \sinh \alpha_i (y_1 - y_2) & \cosh \alpha_i (y_1 - y_2) \end{bmatrix} \begin{bmatrix} U_i(y_2) \\ h \frac{\partial U_i(y_2)}{dy} \end{bmatrix} \tag{9.65}$$

where

$$\begin{aligned} k_i &= \Big(\lambda_i^2 - h^2 k_c^2 \Big)^{1/2} \\ \alpha_i &= \frac{k_i}{h} \,, \quad i = 1, 2, \ldots, N \end{aligned} \tag{9.66}$$

Equation (9.65) can be applied repeatedly to find the transformed potential $[U]$ from one homogeneous layer $y_1 < y < y_2$ to another. Keep in mind that each iteration will require that we recalculate the transformation matrix $[T]$ and its eigenvalues λ_i,

© 2001 by CRC PRESS LLC

which are given in Table 9.1. The field components E_z and H_z are derivable from the scalar potentials $\psi^{(e)}$ and $\psi^{(h)}$ as

$$E_z = \frac{k_c}{j\omega\epsilon}\psi^{(e)} \tag{9.67a}$$

$$H_z = \frac{k_c}{j\omega\mu}\psi^{(h)} \tag{9.67b}$$

To be concrete, consider the shielded microstrip line shown in Fig. 9.8. Because of

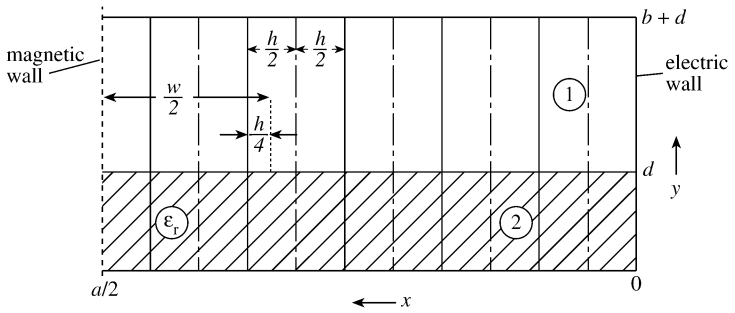

Figure 9.8
Half cross section of a shielded microstrip line.

the symmetry, only half of the solution region needs to be considered. At the interface $y = d$, the continuity conditions with Eq. (9.67) require that

$$\frac{\beta}{\omega\epsilon_o}\frac{\partial}{\partial x}\left(\psi_I^{(e)} - \frac{1}{\epsilon_r}\psi_{II}^{(e)}\right) = \frac{\partial\psi_{II}^{(h)}}{\partial y} - \frac{\partial\psi_I^{(h)}}{\partial y} \tag{9.68}$$

$$\left(k_o^2 - \beta^2\right)\psi_I^{(e)} = \frac{1}{\epsilon_r}\left(\epsilon_r k_o^2 - \beta^2\right)\psi_{II}^{(e)} \tag{9.69}$$

$$\frac{\partial\psi_I^{(h)}}{\partial y} - \frac{\partial\psi_{II}^{(h)}}{\partial y} = \frac{\beta}{\omega\mu}\frac{\partial}{\partial x}\left(\psi_I^{(h)} - \psi_{II}^{(h)}\right) - J_z \tag{9.70}$$

$$\left(k_o^2 - \beta^2\right)\psi_I^{(h)} = \left(\epsilon_r k_o^2 - \beta^2\right)\psi_{II}^{(h)} - j\omega\mu J_x \tag{9.71}$$

where the superscripts I and II refer to dielectric regions 1 and 2 and J_x and J_z are the current densities at the interface $y = d$.

We replace the partial derivative operator $\partial/\partial x$ with the difference operator $[D]$, where

$$[D] = \begin{bmatrix} 1 & -1 & 0 & \dots & 0 \\ 0 & 1 & -1 & \dots & 0 \\ \vdots & \ddots & \ddots & \ddots & \vdots \\ 0 & 0 & \dots & 1 & -1 \end{bmatrix} \tag{9.72}$$

© 2001 by CRC PRESS LLC

so that

$$\begin{aligned}\frac{\partial \psi^{(e)}}{\partial x} &\rightarrow \frac{1}{h}[D][\psi^{(e)}] \\ \frac{\partial \psi^{(h)}}{\partial x} &\rightarrow -\frac{1}{h}[D]^t[\psi^{(h)}]\end{aligned} \tag{9.73}$$

We replace the normal derivatives of $\partial\psi/\partial n$ at the interface $y = d$ with following matrix operators.

$$\begin{aligned}\frac{\partial \psi_k^{(e)}}{\partial n} &\rightarrow \frac{1}{h}\left[G_k^{(e)}\right]\left[\psi_k^{(e)}\right], \qquad k = I, II \\ \frac{\partial \psi_k^{(h)}}{\partial n} &\rightarrow \frac{1}{h}\left[G_k^{(h)}\right]\left[\psi_k^{(h)}\right], \qquad k = I, II\end{aligned} \tag{9.74}$$

We can transform this into the diagonal form

$$\begin{aligned}h\frac{\partial\left[U_k^{(e)}\right]}{\partial n} &= \left[\gamma_k^{(e)}\right]\left[U_k^{(e)}\right], \qquad k = I, II \\ h\frac{\partial\left[U_k^{(h)}\right]}{\partial n} &= \left[\gamma_k^{(h)}\right]\left[U_k^{(h)}\right], \qquad k = I, II\end{aligned} \tag{9.75}$$

With the aid of Eq. (9.65) and the boundary conditions at $y = 0$ and $y = b + d$, the diagonal matrices $[\gamma_k]$ are determined analytically as

$$\begin{aligned}\left[\gamma_I^{(e)}\right] &= \text{diag}\left[\chi_i \coth\left(\chi_i b/h\right)\right] \\ \left[\gamma_I^{(h)}\right] &= \text{diag}\left[\chi_i \tanh\left(\chi_i b/h\right)\right] \\ \left[\gamma_{II}^{(e)}\right] &= \text{diag}\left[\eta_i \coth\left(\eta_i d/h\right)\right] \\ \left[\gamma_{II}^{(h)}\right] &= \text{diag}\left[\eta_i \tanh\left(\eta_i d/h\right)\right]\end{aligned} \tag{9.76}$$

where

$$\chi_i = \left[4\sin^2\left(\frac{i-0.5}{2N+1}\pi\right) - h^2\left(k_o^2 - \beta^2\right)\right]^{1/2} \tag{9.77}$$

and

$$\eta_i = \left[4\sin^2\left(\frac{i-0.5}{2N+1}\pi\right) - h^2\left(\epsilon_r k_o^2 - \beta^2\right)\right]^{1/2} \tag{9.78}$$

We can discretize Eqs. (9.68) to (9.71) and eliminate $\psi_{II}^{(e)}$ and $\psi_{II}^{(h)}$ using $[T^{(e)}]$ and $[T^{(h)}]$ matrices. Equations (9.68) and (9.70) become

$$\frac{\beta}{\omega\epsilon_o}(1-\tau)\left[\delta\right]\left[U_I^{(e)}\right] = \left(\left[\gamma_I^{(h)}\right] + \tau\left[\gamma_{II}^{(h)}\right]\right)\left[U_I^{(h)}\right] \tag{9.79}$$

$$\left(\left[\gamma_I^{(e)}\right] + \epsilon_r\tau\left[\gamma_{II}^{(e)}\right]\right)\left[U_I^{(e)}\right] = \frac{\beta}{\omega\mu}(1-\tau)\left[\delta\right]^t\left[U_I^{(h)}\right] - \left[T^{(e)}\right]^t\left[J_z\right] \tag{9.80}$$

© 2001 by CRC PRESS LLC

where

$$\tau = \frac{1 - \epsilon_{\text{eff}}}{\epsilon_r - \epsilon_{\text{eff}}} \tag{9.81}$$

$$\epsilon_{\text{eff}} = \frac{\beta^2}{k_o^2} \tag{9.82}$$

$$\left[\delta\right] = \left[T^{(h)}\right]^t \left[D\right] \left[T^{(e)}\right] \tag{9.83}$$

and $[T^{(e)}] = [T_{ND}]$ and $[T^{(h)}] = [T_{DN}]$ as given in Table 9.1. Notice that $[\delta]$ is a diagonal matrix and is analytically determined as

$$\delta_i = \text{diag}\left[2 \sin\left(\frac{i - 0.5}{2N + 1}\pi\right)\right] \tag{9.84}$$

Since J_x is negligibly small compared with J_z, we solve Eqs. (9.79) and (9.80) to obtain

$$\left[U_I^{(e)}\right] = \left[\rho\right] \left[T^{(e)}\right]^t \left[J_z\right] \tag{9.85}$$

where

$$\left[\rho\right] = \left[\left[\gamma_I^{(e)}\right] + \epsilon_r \tau \left[\gamma_{II}^{(e)}\right] - \epsilon_{\text{eff}}(1 - \tau)^2 \left[\delta\right]^t \left(\left[\gamma_I^{(h)}\right] + \tau \left[\gamma_{II}^{(h)}\right]\right)^{-1} \left[\delta\right]\right]^{-1} \tag{9.86}$$

which is a diagonal matrix. Using Eq. (9.63), we now take the inverse transform of Eq. (9.85) to obtain

$$\left[\psi_I^{(e)}\right] = \left[T^{(e)}\right] \left[\rho\right] \left[T^{(e)}\right]^t \left[J_z\right] \tag{9.87}$$

We finally impose the boundary condition on the strip, namely

$$\left[\psi_I^{(e)}\right] = \left[0\right] \qquad \text{on the strip} \tag{9.88}$$

which leads to a reduced matrix equation

$$\left[J_z\right] = \begin{cases} \left[J_z\right]_{\text{red}} & \text{on the strip} \\ 0 & \text{elsewhere} \end{cases} \tag{9.89}$$

and the corresponding characteristic equation

$$\left(\left[T^{(e)}\right] \left[\rho\right] \left[T^{(e)}\right]^t\right)_{\text{red}} \left[J_z\right]_{\text{red}} = \left[0\right] \tag{9.90}$$

© 2001 by CRC PRESS LLC

It is known from mathematics that a homogeneous linear matrix equation shows nontrivial solutions only when the determinant of the matrix is equal to zero. Thus the propagation constant is determined by solving the determinant equation

$$\boxed{\det\left(\left[T^{(e)}\right]\left[\rho(\beta,\omega)\right]\left[T^{(e)}f\right]^{t}\right)_{\text{red}} = \left[0\right]} \tag{9.91}$$

The effective dielectric constant ϵ_{eff} is obtained from Eq. (9.82). Notice that only the number of points on the strip determines the size of the matrix and that Eq. (9.91) applies to a microstrip with more than one strip. We solve Eq. (9.91) using a root-finding algorithm [28] in Fortran, Maple, or Matlab. Although a microstrip example is considered here, the formulation is generally valid for any two-layer structures.

Once we solve Eq. (9.91) to determine the effective dielectric constant, the current distribution on the strip, the potential functions ψ_e and ψ_h, the electric field E_z, and magnetic field H_z can be computed. Finally, the characteristic impedance is obtained from

$$Z_o = \frac{2P}{I^2} \tag{9.92}$$

where P is the average power transport along the line

$$P = \frac{1}{2}\int (\mathbf{E}\times\mathbf{H}^*)\cdot dx\,dy\,\mathbf{a}_z \tag{9.93}$$

and I is the total current flowing on the strip

$$I = \int J_z\,dx\,dy \tag{9.94}$$

Since the above analysis applies to multiple strips, the characteristic impedance to the mth strip is

$$Z_{om} = \frac{2P_m}{I_m^2} \tag{9.95}$$

Example 9.4

Consider the shielded microstrip line shown in Fig. 9.8. Using the method of lines, find the effective dielectric constant of the line when $\epsilon_r = 9$, $w/d = 2$, $a/d = 7$, $b/d = 3$ and $d = 1$ mm. □

Solution

The number of lines along the x-axis is selected as $N = 18$ and the number of lines crossing the strip is $M = 6$. These numbers are for only one potential, say $[\psi_e]$. Since only one half of the structure is considered due to symmetry, only three points on the strip are necessary. Hence, the size of the matrix associated with Eq. (9.91) is 3×3.

© 2001 by CRC PRESS LLC

Figure 9.9 shows the three Matlab codes for solving Eq. (9.91). The main program varies the values of d from 0.01 to 0.15, assuming that $\lambda_o = 1$, the wavelength in free space, since β or ϵ_{eff} are frequency-dependent. (Alternatively, we could keep d fixed and vary frequency, from say 1 to 50 GHz.) The program plots ϵ_{eff} with d/λ_o as shown in Fig. 9.10.

(a)

```
%  EXAMPLE 9.4 SOLVED USING METHOD OF LINES
%  THIS M-FILES REQUIRES TWO OTHER M-FILES
%  "FUN.M" AND "ROOT.M" TO WORK
%  FUN.M DETERMINES THE DETERMINANT OF MATRIX [F]
%  ROOT.M FINDS THE ROOT(S) OF THE det(F)
global d

Nmax = 50; tol = 1E-5;
eeff1 = 5; eeff2 = 10;% initial/guessed values
for i=1:15
    d = 0.01*i;
    x(i) = d;
    [eeff] = root('fun', eeff1, eeff2, tol, Nmax)
    y(i) = eeff;
%diary a:test.out
end
diary
  plot(x,y)
diary off
```

Figure 9.9
For Example 9.4: (a) Main Matlab code, *(Continued)*.

The M-file fun.m does the actual computation of the matrices involved using Eq. (9.76) to (9.91). It eventually finds the determinant of matrix $[F]$, where

$$[F] = \left([T_e][\rho(\beta, \omega)][T_e]^t\right)_{\text{red}} \tag{9.96}$$

The third M-file root.m is a root-finding algorithm based on the secant method [28] and is used to determine the value of ϵ_{eff} that will satisfy

$$\det[F] = 0 \tag{9.97}$$

9.3.2 Cylindrical Microstrip Structures

The method of lines can be used to analyze homogeneous and inhomogeneous cylindrical transmission structures [19, 29]–[36] and circular and elliptic waveguides [37]. The principal steps involved in applying MOL in cylindrical coordinates are the same as in Cartesian coordinates. Here, we illustrate with the use of MOL to analyze the dispersion characteristics of the cylindrical microstrip transmission line using full-wave analysis.

We introduce the scalar potentials $\Phi^{(e)}$ and $\Phi^{(h)}$ to represent the electric and magnetic field components. In cylindrical coordinates (ρ, ϕ), the two scalar functions

© 2001 by CRC PRESS LLC

(b)

```
function determinant = fun(eeff)
%  THIS FUNCTION IS NEEDED FOR EXAMPLE 9.4
%  IT DETERMINES THE DETERMINANT OF MATRIX  [F]
%  FOR A GIVEN EFFECTIVE DIELECTRIC CONSTANT EEFF
global d

N = 9;
%d = 0.001;
a = 7*d;  b = 3*d; w = 2*d;
er = 9; h = a/N; M = w/h;
lambdao = 1; %assumed
ko = 2*pi/lambdao;
% First calculate the transformation matrices
% Te (= T_ND) and Th (=T_DN)
cons=sqrt(2/(N+0.5));
for i=1:N
    for j=1:N
        alj = (j - 0.5)*pi/(N + 0.5);
        if (j==1)
            te(i,j) = 1/sqrt(N);
        else
           te(i,j) = cons*cos( (i-0.5)*alj);
        end
    end
end
% Calculate matrices: chi, eta, delta, and gamma
beta = ko*sqrt(eeff);
tau = (1 - eeff)/(er - eeff);
chi = zeros(N,1);
eta = zeros(N,1);
%gammae1 = zeros(N,N)
for i=1:N
x = ((i -0.5)*pi)/(2*N + 1)
chi(i) = sqrt( 4*sin(x)*sin(x) -h^2*(ko^2 - beta^2) );
eta(i) = sqrt( 4*sin(x)*sin(x) -h^2*(er*ko^2 - beta^2) );
 end
 for i=1:N
    for j=1:N
        if(i==j)
            del(i,i) = 2*sin (((i - 0.5)*pi)/(2*N + 1));
            gammae1(i,i) = chi(i)*coth(b*chi(i)/h);
            gammah1(i,i) = chi(i)*tanh(b*chi(i)/h);
            gammae2(i,i) = eta(i)*coth(d*eta(i)/h);
            gammah2(i,i) = eta(i)*tanh(d*eta(i)/h);
        else
            del(i,j) = 0;
            gammae1(i,j) = 0; gammae2(i,j) = 0;
            gammah1(i,j) = 0; gammah2(i,j) = 0;
        end
    end
end
```

Figure 9.9

For Example 9.4: (b) fun M-file for calculating F and its determinant, *(Continued)*.

© 2001 by CRC PRESS LLC

```
% calculate rho matrix
rho = inv(gammae1 + er*tau*gammae2 - eeff*(1 - tau)^2*del'*(inv(gammah1 +
tau*gammah2))*del);
F = [te(1:3,1:3)*rho(1:3,1:3)*te(1:3,1:3)'];
determinant = det(F);
% Next, solve for the root det(X) = 0 using 'root.m'
```

Figure 9.9
For Example 9.4: ***(Cont.)*** **(b) fun M-file for calculating** F **and its determinant,** ***(Continued).***

(c)

```
function [x2] = root(F, x0, x1, tol, Nmax)
% THIS FUNCTION FINDS THE ROOTS OF fun(x) USING
% THE SECANT METHOD
% fun(x) - EXTERNAL FUNCTION THAT COMPUTES THE VALUES OF f(x)
% x0, x1 - LIMITS OF THE INITIAL RANGE
% x2     - ROOT RETURNED TO THE CALLING ROUTINE
% tol    - TOLERANCE VALUE USED IN DETERMINING CONVERGENCE
% Nmax   - MAXIMUM NO. OF ITERATIONS
%
% AUTHORS: M. V. ZEIGLER AND E. CHAMPION [37a]

%F0 = eval( [F, '(x0)']);
F0 = fun(x0);
dx = x1 - x0;
for I=1:Nmax
     F1 = fun(x1);
    %F1 = eval( [F, '(x1)']);
    dx = F1*dx/(F1 - F0);
    x2 = x1 - dx;
% CHECK IF TOLERANCE HAS BEEN MET
    if (abs(dx) <= tol)
    fprintf('root at x = %5.g\n', x2);
    fprintf('root found after this no. of iterations %5.g\n',I);
    break
    end
    dx = x2 - x1;
    x0 = x1;
    x1 = x2;
    F0 = F1;
end
```

Figure 9.9
For Example 9.4: ***(Cont.)*** **(c) root M-file for finding the roots of fun** $(x) = 0$**.**

can be expressed as

$$\Psi^{(e,h)} = \Phi^{(e,h)}(\rho, \phi)e^{-j\beta z} \tag{9.98}$$

where β is the phase constant and the time harmonic dependence has been suppressed. Substituting Eq. (9.98) into the Helmholtz equation for the scalar potential functions

© 2001 by CRC PRESS LLC

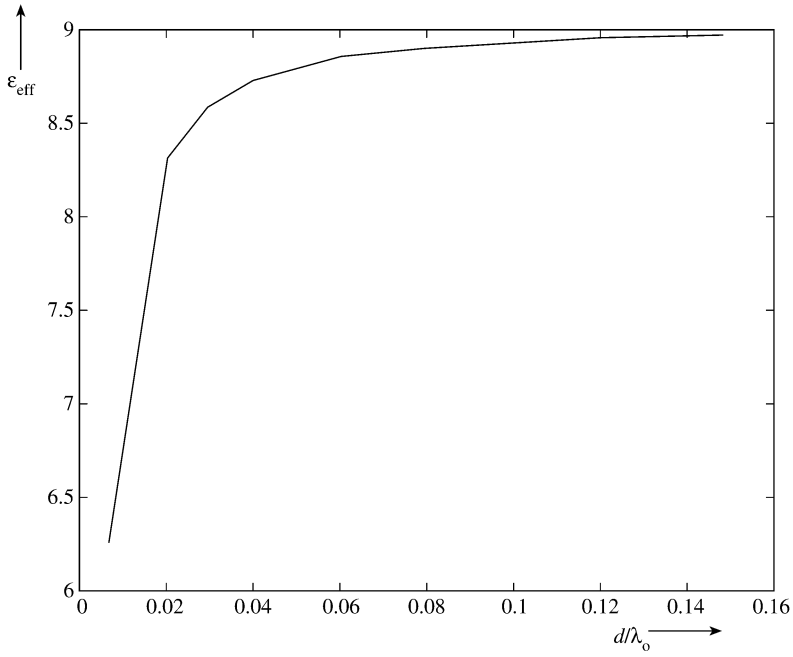

Figure 9.10
For Example 9.4: Effective dielectric constant of the microstrip line.

yields

$$\rho^2 \frac{\partial^2 \Phi}{\partial \rho^2} + \rho \frac{\partial \Phi}{\partial \rho} + \frac{\partial^2 \Phi}{\partial \phi^2} + \rho^2 \left(k^2 - \beta^2\right) \Phi = 0 \tag{9.99}$$

where $k^2 = \omega^2 \mu \epsilon$. Discretizing in the ϕ-direction by using N radial lines, as shown in Fig. 9.11, such that

$$\phi_i = \phi_o + (i-1)h = \frac{2\pi i}{N}, \qquad i = 1, 2, \ldots, N \tag{9.100}$$

where $h = \Delta\phi = 2\pi/N$ is the angular spacing between the lines. The discretization lines for the electric potential function $\Phi^{(e)}$ are shifted from the magnetic potential function $\Phi^{(h)}$ by $h/2$. Applying the central finite difference scheme yields

$$\frac{\partial^2 [\Phi]}{\partial \phi^2} = \frac{[P]}{h^2} [\Phi] \tag{9.101}$$

where

$$[\Phi] = [\Phi_1, \Phi_2, \ldots, \Phi_N]^t \tag{9.102}$$

© 2001 by CRC PRESS LLC

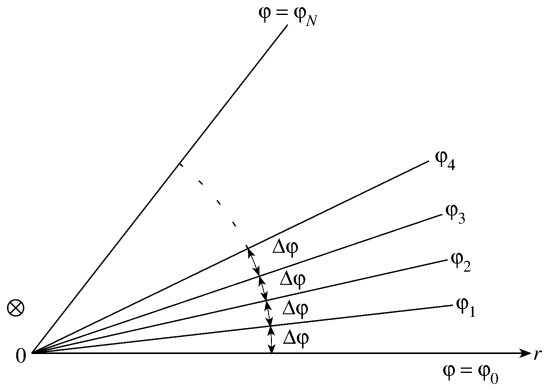

Figure 9.11
Discretization in the ϕ-direction.

and $[P]$ is given in Eq. (9.34). Introducing Eq. (9.101) into Eq. (9.99) leads to N coupled differential equations:

$$\rho^2 \frac{\partial^2[\Phi]}{\partial \rho^2} + \rho \frac{\partial[\Phi]}{\partial \rho} + \rho^2 k_c^2 [\Phi] - \frac{[P]}{h^2}[\Phi] = 0 \tag{9.103}$$

where $k_c^2 = k^2 - \beta^2$ and $[P]$ is the same as in Eq. (9.34) if ϕ goes from 0 to 2π otherwise $[P]$ is as in Eq. (9.7). Here we will assume $[P]$ in Eq. (9.7). To decouple Eq. (9.103), we must diagonalize $[P]$ by an orthogonal matrix $[T]$ given in Eq. (9.38) and introduce the transformed potential U that satisfies

$$[U] = [T][\Phi] \tag{9.104}$$

Thus Eq. (9.103) becomes

$$\rho^2 \frac{\partial^2[U]}{\partial \rho^2} + \rho \frac{\partial[U]}{\partial \rho} + \left[k_c^2 \rho^2 - \mu_i^2\right][U] = 0 \tag{9.105}$$

where

$$[U] = [U_1, U_2, \ldots, U_N]^t \tag{9.106}$$

is a vector containing the transformed potential function and

$$\mu_i = \frac{\lambda_i}{h} \tag{9.107}$$

We notice that Eq. (9.105) is essentially a Bessel equation and can be solved for every homogeneous region to produce Bessel function of order μ_n. The solution is

$$U_i(\rho) = A_i J_{\mu i}(k_c \rho) + B_i Y_{\mu i}(k_c \rho)\,, \quad i = 1, 2, \ldots, N \tag{9.108}$$

© 2001 by CRC PRESS LLC

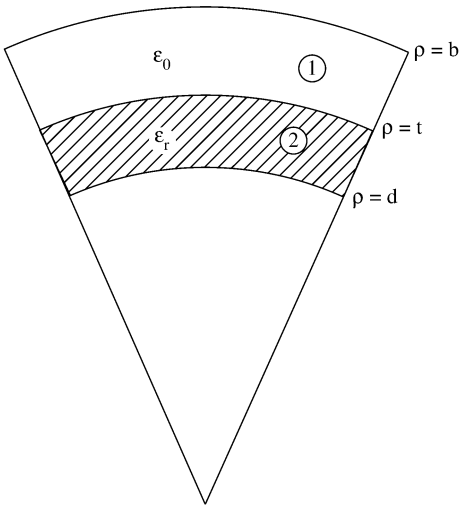

Figure 9.12
The cross section of a shielded cylindrical microstrip line.

where J and Y are Bessel functions of the first and second kind, respectively.

To be concrete, consider the cross section of a shield cylindrical microstrip line shown in Fig. 9.12. Due to the symmetry of the structure, we need only consider half the cross section as in Fig. 9.13. We have regions I and II and we apply Eq. (9.108) to each region. On the boundaries $\rho = d$ and $\rho = b$ (electric walls), we have the boundaries conditions

$$\begin{aligned} U_{Ii}^{(e)}(\rho = d) &= 0 \\ U_{IIi}^{(e)}(\rho = b) &= 0 \end{aligned} \tag{9.109}$$

Enforcing Eq. (9.109) on Eq. (9.108), we obtain

$$\begin{aligned} 0 &= A_i J_{\mu_i}(k_c d) + B_i Y_{\mu_i}(k_c d) \ , \\ 0 &= C_i J_{\mu_i}\left(k_c' b\right) + D_i Y_{\mu_i}\left(k_c' b\right) \end{aligned} \tag{9.110}$$

where $k_c = \sqrt{k_o^2 - \beta^2}$ and $k_c' = \sqrt{\epsilon_r k_o^2 - \beta^2}$, $k_o = 2\pi/\lambda_o$, and λ_o is the wavelength in free space. From Eq. (9.110),

$$\begin{aligned} \frac{B_i}{A_i} &= -\frac{J_{\mu_i}(k_c d)}{Y_{\mu_i}(k_c d)} \\ \frac{D_i}{C_i} &= -\frac{J_{\mu_i}(k_c' b)}{Y_{\mu_i}(k_c' b)} \end{aligned} \tag{9.111}$$

© 2001 by CRC PRESS LLC

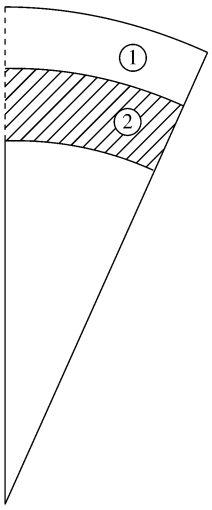

Figure 9.13
Half the cross section of the microstrip in Fig. 9.12 (— electric wall; - - - magnetic wall).

For $\Phi^{(h)}$, the boundary conditions are

$$\left.\frac{\partial U_{Ii}^{(h)}}{\partial \rho}\right|_{\rho=d} = 0$$
$$\left.\frac{\partial U_{IIi}^{(h)}}{\partial \rho}\right|_{\rho=b} = 0 \tag{9.112}$$

Enforcing this on Eq. (9.108) yields

$$0 = E_i J'_{\mu_i}(k_c d) + F_i Y'_{\mu_i}(k_c d) \ ,$$
$$0 = G_i J'_{\mu_i}(k'_c \rho) + H_i Y'_{\mu_i}\left(k'_c b\right) \ , \tag{9.113}$$

which leads to

$$\frac{F_i}{E_i} = -\frac{J'_{\mu_i}(k_c d)}{Y'_{\mu_i}(k_c d)}$$
$$\frac{H_i}{G_i} = -\frac{J'_{\mu_i}(k'_c b)}{Y'_{\mu_i}(k'_c b)} \tag{9.114}$$

At the interface $\rho = t$, both $\Phi^{(e)}$ and $\Phi^{(h)}$ are related by the continuity conditions of

© 2001 by CRC PRESS LLC

the tangential components of the electric and magnetic fields. Since

$$\Phi^{(e)} = \frac{j\omega\epsilon_o\epsilon_r}{k_o^2\epsilon_r - \beta^2} E_z$$
$$\Phi^{(h)} = \frac{j\omega\mu_r}{k_o^2\epsilon_r - \beta^2} H_z \tag{9.115}$$

the continuity conditions are

$$\frac{1}{t}\frac{\beta}{\omega\epsilon_o}\frac{\partial}{\partial\phi}\left(\Phi_I^{(e)} - \frac{1}{\epsilon_r}\Phi_{II}^{(e)}\right) = \frac{\partial\Phi_{II}^{(h)}}{\partial\rho} - \frac{\partial\psi_I^{(h)}}{\partial\rho} \tag{9.116}$$

$$\left(k_o^2 - \beta^2\right)\psi_I^{(e)} = \frac{1}{\epsilon_r}\left(\epsilon_r k_o^2 - \beta^2\right)\psi_{II}^{(e)} \tag{9.117}$$

$$\frac{\partial\Phi_I^{(h)}}{\partial\rho} - \frac{\partial\Phi_{II}^{(h)}}{\partial\rho} = \frac{\beta}{\omega\mu_o t}\frac{\partial}{\partial\phi}\left(\Phi_I^{(h)} - \Phi_{II}^{(h)}\right) - J_z \tag{9.118}$$

$$\left(k_o^2 - \beta^2\right)\psi_I^{(h)} = \left(\epsilon_r k_o^2 - \beta^2\right)\psi_{II}^{(h)} - j\omega\mu J_\phi \tag{9.119}$$

As we did in Section 9.3.1, we replace the derivative operator $\partial/\partial\phi$ with the difference operator $[D]$ and transform the resulting equations into the diagonal matrices. We obtain the elements of the diagonal matrices as [30]

$$\gamma_{Ii}^{(e)} = S_o h\left[\frac{J'_{\mu_i}(S_o) + (B_i/A_i)Y'_{\mu_i}(S_o)}{J_{\mu_i}(S_o) + (B_i/A_i)Y_{\mu_i}(S_o)}\right] \tag{9.120a}$$

$$\gamma_{IIi}^{(e)} = -S'_o h\left[\frac{J'_{\mu_i}(S'_o) + (D_i/C_i)Y'_{\mu_i}(S'_o)}{J_{\mu_i}(S'_o) + (D_i/C_i)Y_{\mu_i}(S'_o)}\right] \tag{9.120b}$$

$$\gamma_{Ii}^{(h)} = S_o h\left[\frac{J'_{\mu_i}(S_o) + (F_i/E_i)Y'_{\mu_i}(S_o)}{J_{\mu_i}(S_o) + (F_i/E_i)Y_{\mu_i}(S_o)}\right] \tag{9.120c}$$

$$\gamma_{IIi}^{(h)} = -S'_o h\left[\frac{J'_{\mu_i}(S'_o) + (H_i/G_i)Y'_{\mu_i}(S'_o)}{J_{\mu_i}(S'_o) + (H_i/G_i)Y_{\mu_i}(S'_o)}\right] \tag{9.120d}$$

where $h = \Delta\phi$ and

$$S_o = t\sqrt{k_o^2 - \beta^2}\,, \quad S'_o = t\sqrt{k_o^2\epsilon - \beta^2} \tag{9.121}$$

By ignoring J_ϕ and reducing J_z to what we have in Eq. (9.89), we finally obtain the characteristic equation

$$\left(\left[T^{(e)}\right]\left[\rho\right]\left[T^{(e)}\right]^t\right)_{\text{red}}\left[J_z\right]_{\text{red}} = [0] \tag{9.122}$$

© 2001 by CRC PRESS LLC

where

$$\left[\rho\right] = \left[\left[\gamma_I^{(e)}\right] + \epsilon_r \tau \left[\gamma_{II}^{(e)}\right] - \epsilon_{\text{eff}}(1-\tau)^2 \left[\delta\right]^t \left(\left[\gamma_I^{(h)}\right] + \tau \left[\gamma_{II}^{(h)}\right]\right)^{-1} \left[\delta\right]\right]^{-1} \quad (9.123)$$

$$\tau = \frac{1-\epsilon_{\text{eff}}}{\epsilon_r - \epsilon_{\text{eff}}}\,, \quad \epsilon_{\text{eff}} = \frac{\beta^2}{k_o^2}\,, \quad \left[\delta\right] = \left[T^{(h)}\right]^t \left[D\right] \left[T^{(e)}\right] \quad (9.124)$$

With a root-finding algorithm, Eq. (9.122) can be solved to obtain β or ϵ_{eff}. Notice that Eq. (9.122) is of the same form as Eq. (9.90) and only the number of points on the strip determines the size of the matrix. However, the expressions for $[\gamma_I^{(e)}]$, $[\gamma_{II}^{(e)}]$, $[\gamma_I^{(h)}]$ and $[\gamma_{II}^{(h)}]$ are given in Eq. (9.120).

9.4 Time-Domain Solution

The frequency-domain version of the method of lines covered in Section 9.3 can be extended to the time-domain [38]–[43]. In fact, MOL can also be used to solve parabolic equations [1, 44, 45]. However, in this section, we will use MOL to solve hyperbolic Maxwell's equations in the time-domain. Essentially, the MOL proceeds by leaving the derivatives along one selected axis untouched (usually in time), while all other partial derivatives (usually in space) are discretized using well-known techniques such as finite difference and finite element. The partial differential equation is reduced to a system of ordinary differential equations that can be solved numerically using standard methods.

Consider an empty rectangular waveguide which is infinite in the z-direction [38] and with cross-section $0 < x < a$, $0 < y < b$. We assume that the waveguide is excited by a uniform electric field E_z. The problem becomes a two-dimensional one. It corresponds to calculating the cutoff frequencies of various modes in the frequency-domain. Such information can be obtained from the time-domain data.

Due to the excitation, only E_z, H_x, and H_y exist and $\partial/\partial z = 0$. Maxwell's equations become

$$\begin{aligned} -\mu \frac{\partial H_x}{\partial t} &= \frac{\partial E_z}{\partial y} \\ \mu \frac{\partial H_y}{\partial t} &= \frac{\partial E_z}{\partial x} \\ \epsilon \frac{\partial E_z}{\partial t} &= \frac{\partial H_y}{\partial x} - \frac{\partial H_x}{\partial y} \end{aligned} \quad (9.125)$$

which can be manipulated to yield the wave equation

$$\frac{\partial^2 E_z}{\partial^2 x} + \frac{\partial^2 E_z}{\partial^2 y} - \mu\epsilon \frac{\partial^2 E_z}{\partial^2 t} = 0 \quad (9.126)$$

© 2001 by CRC PRESS LLC

Discretizing in the x-direction only leads to

$$-\mu\frac{\partial\left[H_x\right]}{\partial t} = \frac{\partial\left[E_z\right]}{\partial y} \tag{9.127a}$$

$$\mu\frac{\partial\left[H_y\right]}{\partial t} = \frac{\left[D_x^{(e)}\right]\left[E_z\right]}{\Delta x} \tag{9.127b}$$

$$\epsilon\frac{\partial\left[E_z\right]}{\partial t} = \frac{\left[\Delta_x^{(h)}\right]\left[H_y\right]}{\Delta x} - \frac{\partial\left[H_x\right]}{\partial y} \tag{9.127c}$$

$$\frac{\left[D_{xx}^{(e)}\right]\left[E_z\right]}{(\Delta x)^2} + \frac{\partial^2\left[E_z\right]}{\partial^2 y} - \mu\epsilon\frac{\partial^2\left[E_z\right]}{\partial^2 t} = 0 \tag{9.127d}$$

where $[E_z]$, $[H_x]$, and $[H_y]$ are column vectors representing the fields along each line and are functions of y and t. As given in Section 9.3.1, matrices $[D_x^{(e)}]$, $[D_x^{(h)}]$, and $[D_{xx}^{(e)}]$ represent difference operators in which the boundary conditions at the side walls are incorporated.

Due to the fact that $[D_{xx}^{(e)}]$ is a real symmetric matrix, there exists a real orthogonal matrix $[T_x^{(e)}]$ that transforms $[D_{xx}^{(e)}]$ into a diagonal matrix $[\lambda^2]$. We can transform $[E_z]$ into a transform

$$\left[\overline{E}_z\right] = \left[T_x^{(e)}\right]\left[E_z\right] \tag{9.128}$$

(and similarly $[H_x]$ and $[H_y]$) so that Eq. (9.127d) becomes

$$\frac{\left[\lambda^2\right]\left[E_z\right]}{(\Delta x)^2} + \frac{\partial^2\left[\overline{E}_z\right]}{\partial^2 y} - \mu\epsilon\frac{\partial^2\left[\overline{E}_z\right]}{\partial^2 t} = 0 \tag{9.129}$$

This is a set of uncoupled partial differential equations. The solution for the ith line is

$$\overline{E}_{zi}(y,t) = \sum_n \left(A_{ni}\cos\omega_{ni}t + B_{ni}\sin\omega_{ni}t\right)\sin\alpha_n y \tag{9.130}$$

where

$$\begin{aligned}\omega_{ni} &= \frac{u}{\sqrt{(n\pi/b)^2 - \lambda_i^2/(\Delta x)^2}}\\ \alpha_n &= n\pi/b\end{aligned} \tag{9.131}$$

and $u = 1/\sqrt{\mu\epsilon}$ is the wave velocity. Given the initial conditions for $\overline{E}_z$ and its time derivative, we can find A_{ni} and B_{ni}. The solution at any point at any time can be extracted from Eqs. (9.130) and (9.127a), (9.127b), and (9.127c) and the subsequent inverse transforms such as

$$\left[E_z(y,t)\right] = \left[T_x^{(e)}\right]\left[\overline{E}_z\right] \tag{9.132}$$

This completes the solution process.

© 2001 by CRC PRESS LLC

9.5 Concluding Remarks

The method of lines (MOL) is a differential-difference approach of solving elliptic, parabolic, and hyperbolic PDEs. It involves a judicious combination of analysis and computation. Given a partial differential equation, all but one of the independent variables are discretized to obtain a system of ordinary differential equations.

MOL requires that the structures be at least piecewise uniform in one dimension. Also, the eigenmatrices and eigenvalues depend on the boundaries of the solution region. These requirements have limited the applications of the method. Although not applicable to problems with complex geometries, the method of lines has been efficient for the analysis of compatible planar structures. Applications of the method include but are not limited to the following EM-related problems:

- waveguides including optical types [46]–[65],
- planar and cylindrical microstrip transmission lines [19]–[27, 66, 67],
- scattering from discontinuities in planar structures [39, 40, 68],
- antennas [32],
- electro-optic modulator structures [17, 69, 70], and
- other areas [71]–[75]

Originally, MOL was developed for problems with closed solution domain. Recently, absorbing boundary conditions appropriate for MOL have been introduced [51, 76]–[78]. With these conditions, it is now possible to simulate and model unbounded electromagnetic structures. The equivalence between the method of lines and variational method is given in [79].

References

[1] A. Zafarullah, "Application of the method of lines to parabolic partial differential equation with error estimates," *Jour. ACM,* vol. 17, no. 2, Apr. 1970, pp. 294–302.

[2] M.B. Carver and H.W. Hinds, "The method of lines and the advection equation," *Simulation,* vol. 31, no. 2, 1978, pp. 59–69.

[3] W.E. Schiesser, *The Numerical Method of Lines.* San Diego: Academic Press, 1991.

© 2001 by CRC PRESS LLC

[4] G.H. Meyer, "The method of lines for Poisson's equation with nonlinear or free boundary conditions," *Numer. Math.,* vol. 29, 1978, pp. 329–344.

[5] V.N. Sushch, "Difference Poisson equation on a curvilinear mesh," *Diff. Equations,* vol. 12, no. 5, 1996, pp. 693–697.

[6] O.A. Liskovets, "The method of lines (review)," *Differential Equations,* vol. 1, no. 12, 1965, pp. 1308–1323.

[7] R. Pregla and W. Pascher, "The method of lines," in T. Itoh (ed.), *Numerical Techniques for Microwave and Millimeter-wave passive structures*. New York: John Wiley, 1989, pp. 381–446.

[8] R. Pregla, "Analysis of planar microwave structures on magnetized ferrite substrate," *Arch. Elek. Ubertragung.,* vol. 40, 1986, pp. 270–273.

[9] R. Pregla, "About the nature of the method of lines," *Arch. Elek. Ubertragung.,* vol. 41, no. 6, 1987, pp. 368–370.

[10] R. Pregla, "Higher order approximation for the difference operators in the method of lines," *IEEE Micro. Guided Wave Lett.,* vol. 5, no. 2, Feb. 1995, pp. 53–55.

[11] U. Schulz and R. Pregla, "A new technique for the analysis of the dispersion characteristics of planar waveguides," *Arch. Elek. Ubertragung.,* vol. 34, Apr. 1980, pp. 169–173. Also in R. Sorrentino (ed.), *Numerical Methods for Passive Microwave and Millimeter Wave Structure,* New York: IEEE Press, 1989, pp. 233–237.

[12] U. Schulz and R. Pregla, "A new technique for the analysis of the dispersion characteristics of planar waveguides and its application to microstrips with tuning septums," *Radio Sci.,* vol. 16, Nov./Dec. 1981, pp. 1173–1178.

[13] R. Pregla and W. Pascher, "Diagonalization of difference operators and system matrices in the method of lines," *IEEE Micro. Guided Wave Lett.,* vol. 2, no. 2, Feb. 1992, pp. 52–54.

[14] A. Dreher and T. Rother, "New aspects of the method of lines," *IEEE Micro. Guided Wave Lett.,* vol. 5, no. 11, Nov. 1995, pp. 408–410.

[15] D.J. Jones et al., "On the numerical solution of elliptic partial differential equations by the method of lines," *Jour. Comp. Phys.,* vol. 9, 1972, pp. 496–527.

[16] B.H. Edwards, "The numerical solution of elliptic differential equation by the method of lines," *Revista Colombiana de Matematicas,* vol. 19, 1985, pp. 297–312.

[17] A.G. Keen et al., "Quasi-static analysis of electrooptic modulators by the method of lines," *J. Lightwave Tech.,* vol. 8, no. 1, Jan. 1990, pp. 42–50.

[18] J.G. Ma and Z. Chen, "Application of the method of lines to the Laplace equation," *Micro. Opt. Tech. Lett.,* vol. 14, no. 6, 1997, pp. 330–333.

© 2001 by CRC PRESS LLC

[19] S. Xiao et al., " Analysis of cylindrical transmission lines with the method of lines," *IEEE Trans. Micro. Theo. Tech.,* vol. 44, no. 7, July 1996, pp. 993–999.

[20] H. Diestel, "Analysis of planar multiconductor transmission-line system with the method of lines," *AEU,* vol. 41, 1987, pp. 169–175.

[21] Z. Chen and B. Gao, "Full-wave analysis of multiconductor coupled lines in MICs by the method of lines," *IEEE Proc.,* Pt. H, vol. 136, no. 5, Oct. 1989, pp. 399–404.

[22] W. Pascher and R. Pregla, "Full wave analysis of complex planar microwave structures," *Radio Sci.,* vol. 22, no. 6, Nov. 1987, pp. 999–1002.

[23] M.A. Thorburn et al., "Application of the method of lines to planar transmission lines in waveguides with composite cross-section geometries," *IEEE Proc.,* Pt. H, vol. 139, no. 6, Dec. 1992, pp. 542–544.

[24] R. Pregla, "Analysis of a microstrip bend discontinuity by the method of lines," *Frequenza,* vol. 145, 1991, pp. 213–216.

[25] Y.J. He and S.F. Li, "Analysis of arbitrary cross-section microstrip using the method of lines," *IEEE Trans. Micro. Theo. Tech.,* vol. 42, no. 1, Jan. 1994, pp. 162–164.

[26] M. Thorburn et al., "Computation of frequency-dependent propagation characteristics of microstriplike propagation structures with discontinuous layers," *IEEE Trans. Micro. Theo. Tech.,* vol. 38, no. 2, Feb. 1990, pp. 148–153.

[27] P. Meyer and P.W. van der Walt, "Closed-form expression for implementing the method of lines for two-layer boxed planar structures," *Elect. Lett.,* vol. 30, no. 18, Sept. 1994, pp. 1497–1498.

[28] E.R. Champion, *Numerical methods for Engineering Applications*. New York: Marcel Dekker, 1993, pp. 196–215.

[29] L. Urshev and A. Stoeva, "Application of equivalent transmission line concept to the method of lines," *Micro. Opt. Tech. Lett.,* vol. 3, no. 10, Oct. 1990, pp. 341–343.

[30] Y. Xu, "Application of method of lines to solve problems in the cylindrical coordinates," *Micro. Opt. Tech. Lett.,* vol. 1, no. 5, May 1988, pp. 173–175.

[31] K. Gu and Y. Wang, "Analysis of dispersion characteristics of cylindrical microstrip line with method of lines," *Elect. Lett.,* vol. 26, no. 11, May 1990, pp. 748–749.

[32] R. Pregla, "New approach for the analysis of cylindrical antennas by the method of lines," *Elect. Lett.,* vol. 30, no. 8, April 1994, pp. 614–615.

[33] R. Pregla, "General formulas for the method of lines in cylindrical coordinates," *IEEE Trans. Micro. Theo. Tech.,* vol. 43, no. 7, July 1995, pp. 1617–1620.

© 2001 by CRC PRESS LLC

[34] R. Pregla, "The method of lines for the analysis of dielectric waveguide bends," *J. Lightwave Tech.,* vol. 14, no. 4, 1996, pp. 634–639.

[35] D. Kremer and R. Pregla, "The method of lines for the hybrid analysis of multilayered cylindrical resonator structures," *IEEE Trans. Micro. Theo. Tech.,* vol. 45, no. 12, Dec. 1997, pp. 2152–2155.

[36] M. Thorburn et al., " Application of the method of lines to cylindrical inhomogeneous propagation structures," *Elect. Lett.,* vol. 26, no. 3, Feb. 1990, pp. 170–171.

[37] K. Wu and R. Vahldieck, "The method of lines applied to planar transmission lines in circular and elliptical waveguides," *IEEE Trans. Micro. Theo. Tech.,* vol. 37, no. 12, Dec. 1989, pp. 1958–1963.

[38] S. Nam et al., "Time-domain method of lines," *Elect. Lett.,* vol. 24, no. 2, Jan. 1988, pp. 128–129.

[39] S. Nam et al., "Time-domain method of lines applied to planar waveguide structures," *IEEE Trans. Micro. Theo. Tech.,* vol. 37, 1989, pp. 897–901.

[40] S. Nam et al., "Characterization of uniform microstrip line and its discontinuities using the time-domain method of lines," *IEEE Trans. Micro. Theo. Tech.,* vol. 37, 1989, pp. 2051–2057.

[41] H. Zhao et al., "Numerical solution of the power density distribution generated in a multimode cavity by using the method of lines technique to solve directly for the electric field," *IEEE Trans. Micro. Theo. Tech.,* vol. 44, no. 12, Dec. 1996, pp. 2185–2194.

[42] W. Fu and A. Metaxas, "Numerical prediction of three-dimensional power density distribution in a multi-mode cavity," *Jour. Micro. Power Electromag. Energy,* vol. 29, no. 2, 1994, pp. 67–75.

[43] W.B. Fu and A.C. Metaxas, "Numerical solution of Maxwell's equations in three dimensions using the method of lines with applications to microwave heating in a multimode cavity," *Int. Jour. Appl. Engr. Mech.,* vol. 6, 1995, pp. 165–186.

[44] J. Lawson and M. Berzins, "Towards an automatic algorithm for the numerical solution of parabolic partial differential equations using the method of lines," in J. R. Cash and I. Gladwell (eds.), *Computational Ordinary Differential Equations*. Oxford: Clarendon Press, 1992, pp. 309–322.

[45] B. Zubik-Kowal, "The method of lines for parabolic differential-functional equations," *IMA Jour. Num. Analy.,* vol. 17, 1997, pp. 103–123.

[46] W. Pascher and R. Pregla, "Analysis of rectangular waveguide junctions by the method of lines," *IEEE Trans. Micro. Theo. Tech.,* vol. 43, no. 12, Dec. 1993, pp. 2649–2653.

© 2001 by CRC PRESS LLC

[47] S.J. Chung and T.R. Chrang, "Full-wave analysis of discontinuities in conductor-backed coplanar waveguides using the method of lines," *IEEE Trans. Micro. Theo. Tech.,* vol. 41, no. 9, 1993, pp. 1601–1605.

[48] A. Papachristoforos, "Method of lines for analysis of planar conductors with finite thickness," *IEEE Proc. Micro. Ant. Prog.,* vol. 141, no. 3, June 1994, pp. 223–228.

[49] R. Pregla and W. Yang, "Method of lines for analysis of multilayered dielectric waveguides with Bragg grating," *Elect. Lett.,* vol. 29, no. 22, Oct. 1993, pp. 1962–1963.

[50] R.R. Kumar et al., "Modes of a shielded conductor-backed coplanar waveguide," *Elect. Lett.,* vol. 30, no. 2, Jan. 1994, pp. 146–147.

[51] A. Dreher and R. Pregla, "Full-wave analysis of radiating planar resonators with the method of lines," *IEEE Trans. Micro. Theo. Tech.,* vol. 41, no. 8, Aug. 1993, pp. 1363–1368.

[52] U. Rogge and R. Pregla, "Method of lines for the analysis of strip-load optical waveguide," *J. Opt. Soc. Amer. B,* vol. 8, no. 2, pp. 463–489.

[53] F.J. Schmuckle and R. Pregla, "The method of lines for the analysis of lossy planar waveguides," *IEEE Trans. Micro. Theo. Tech.,* vol. 38, no. 10, Oct. 1990, pp. 1473–1479.

[54] F.J. Schmuckle and R. Pregla, "The method of lines for the analysis of planar waveguides with finite metallization thickness," *IEEE Trans. Micro. Theo. Tech.,* vol. 39, no. 1, Jan. 1991, pp. 107–111.

[55] R.S. Burton and T.E. Schlesinger, "Least squares technique for improving three-dimensional dielectric waveguide analysis by the method of lines," *Elect. Lett.,* vol. 30, no. 13, June 1994, pp. 1071–1072.

[56] R. Pregla and E. Ahlers, "Method of lines for analysis of arbitrarily curved waveguide bends," *Elect. Lett.,* vol. 30, no. 18, Sept. 1994, pp. 1478–1479.

[57] R. Pregla and E. Ahlers, "Method of lines for analysis of discontinuities in optical waveguides," *Elect. Lett.,* vol. 29, no. 21, Oct. 1993, pp. 1845–1846.

[58] J.J. Gerdes, "Bidirectional eigenmode propagation analysis of optical waveguides based on method of lines," *Elect. Lett.,* vol. 30, no. 7, March 1994, pp. 550–551.

[59] S.J. Al-Bader and H.A. Jamid, "Method of lines applied to nonlinear guided waves," *Elect. Lett.,* vol. 31, no. 17, Aug. 1995, pp. 1455–1457.

[60] W.D. Yang and R. Pregla, "Method of lines for analysis of waveguide structures with multidiscontinuities," *Elect. Lett.,* vol. 31, no. 11, May 1995, pp. 892–893.

[61] J. Gerdes et al., "Three-dimensional vectorial eigenmode algorithm for non-paraxal propagation in reflecting optical waveguide structures," *Elect. Lett.,* vol. 31, no. 1, Jan. 1995, pp. 65–66.

© 2001 by CRC PRESS LLC

[62] W. Pascher and R. Pregla, "Vectorial analysis of bends in optical strip waveguides by the method of lines," *Radio Sci.,* vol. 28, no. 6, Nov./Dec. 1993, pp. 1229–1233.

[63] S.B. Worm, "Full-wave analysis of discontinuities in planar waveguides by the method of lines using a source approach," *IEEE Trans. Micro. Theo. Tech.,* vol. 38, no. 10, Oct. 1990, pp. 1510–1514.

[64] S.J. Al-Bader and H.A. Jamid, "Mode scattering by a nonlinear step-discontinuity in dielectric optical waveguide," *IEEE Trans. Micro. Theo. Tech.,* vol. 44, no. 2, Feb. 1996, pp. 218–224.

[65] S.J. Chung and L.K. Wu, "Analysis of the effects of a resistively coated upper dielectric layer on the propagation characteristics of hybrid modes in a waveguide-shielded microstrip using the method of lines," *IEEE Trans. Micro. Theo. Tech.,* vol. 41, no. 8, Aug. 1993, pp. 1393–1399.

[66] M.J. Webster et al., "Accurate determination of frequency dependent three element equivalent circuit for symmetric step microstrip discontinuity," *IEEE Proc.,* vol. 137, Pt. H, no. 1, Feb. 1990, pp. 51–54.

[67] Y. Chen and B. Beker, "Study of microstrip step discontinuities on bianisotropic substrates using the method of lines and transverse resonance technique," *IEEE Trans. Micro. Theo. Tech.,* vol. 42, no. 10, Oct. 1994, pp. 1945–1950.

[68] P. Meyer, "Solving microstrip discontinuities with a combined mode-matching and method-of-lines procedure," *Micro. Opt. Tech. Lett.,* vol. 8, no. 1, Jan. 1995, pp. 4–8.

[69] J. Gerdes et al., "Full wave analysis of traveling-wave electrodes with finite thickness for electro-optic modulators by the method of lines," *Jour. Lightwave Tech.,* vol. 9, no. 4, Aug. 1991, pp. 461–467.

[70] S.J. Chung, "A 3-dimensional analysis of electrooptic modulators by the method of lines," *IEEE Trans. Mag.,* vol. 29, no. 2, March 1993, pp. 1976–1980.

[71] A. Kormatz and R. Pregla, "Analysis of electromagnetic boundary-value problems in inhomogeneous media with the method of lines," *IEEE Trans. Micro. Theo. Tech.,* vol. 44, no. 12, Dec. 1996, pp. 2296–2299.

[72] B.M. Sherrill and N.G. Alexopoulos, "The method of lines applied to a finline/strip configuration on an anisotropic subtrate," *IEEE Trans. Micro. Theo. Tech.,* vol. 35, no. 6, June 1987, pp. 568–574.

[73] L. Vietzorreck and R. Pregla, "Hybrid analysis of three-dimensional MMIC elements by the method of lines," *IEEE Trans. Micro. Theo. Tech.,* vol. 44, no. 12, Dec. 1996, pp. 2580–2586.

[74] K. Suwan and A. Anderson, "Method of lines applied to Hyperbolic fluid transient equations," *Int. Jour. Num. Methods Engr.,* vol. 33, 1992, pp. 1501–1511.

© 2001 by CRC PRESS LLC

[75] A.G. Bratsos, "The solution of the Boussinesq equation using the method of lines," *Comp. Methods Appl. Mech. Engr.,* vol. 157, 1998, pp. 33–44.

[76] A. Dreher and R. Pregla, "Analysis of planar waveguides with the method of lines and absorbing boundary conditions," *IEEE Micro. Guided Wave Lett.,* vol. 1, no. 6, June 1991, pp. 138–140.

[77] R. Pregla, and L. Vietzorreck, "Combination of the source method with absorbing boundary conditions in the method of lines," *IEEE Micro. Guided Wave Lett.,* vol. 5, no. 7, July 1995, pp. 227–229.

[78] K. Wu and X. Jiang, "The use of absorbing boundary conditions in the method of lines," *IEEE Micro. Guided Wave Lett.,* vol. 6, no. 5, May 1996, pp. 212–214.

[79] W. Hong and W.X. Zhang, "On the equivalence between the method of lines and the variational method," *AEU,* vol. 45, no. 1, 1991, pp. 198–201.

Problems

9.1 In Eq. (9.7), show that $p_\ell = 2$ for Dirichlet condition and $p_\ell = 1$ for Neumann condition.

9.2 If the first-order finite difference scheme can be written as

$$h\frac{\partial[V]}{\partial x} \simeq -[D_x]^t\,[V]$$

where the equidistance difference matrix $[D_x]$ is an $(N-1)\times N$ matrix given by

$$[D_x] = \begin{bmatrix} 1 & -1 & & \\ & \ddots & \ddots & \\ & & 1 & -1 \end{bmatrix}$$

show that the central finite difference scheme for second-order partial differential operator yields

$$h^2\frac{\partial^2[V]}{\partial x^2} \simeq [D_{xx}]\,[V]$$

where $[D_{xx}] = -[D_x]^t[D_x] = -[D_x][D_x]^t$. Assume Neumann conditions at both side walls and obtain D_{xx}.

9.3 Obtain the transformation matrix $[T]$ and its corresponding eigenvalue matrix $[\lambda^2]$ for Neumann-Dirichlet boundary conditions. Assume that $t_0^{(k)} - t_1^{(k)} = 0$ and $t_{N+1}^{(k)} = 0$ on the boundaries.

© 2001 by CRC PRESS LLC

9.4 Using MOL, solve Laplace's equation

$$\nabla^2 \Phi = 0$$

in a rectangular domain $0 \le x \le 1$, $-1 \le y \le 1$ with the following Dirichlet boundary conditions:

$$\Phi(0, y) = \Phi(1, y) = 0$$
$$\Phi(x, 1) = \Phi(x, -1) = \sin \pi x$$

Obtain Φ at $(0, 0.5)$, $(0.5, 0.25)$, $(0.5, 0.5)$, $(0.5, 0.75)$. Compare your solution with the exact solution

$$\Phi(x, y) = \frac{\cosh(\pi y) \sin(\pi x)}{\cosh(\pi b)}$$

9.5 Obtain the solution of Prob. 2.4(a) using MOL.

9.6 Consider the coaxial cable of elliptical cylindrical cross section shown in Fig. 9.14. Take $A = 2$ cm, $B = 2$ cm, $a = 1$ cm, and $b = 2$ cm. For

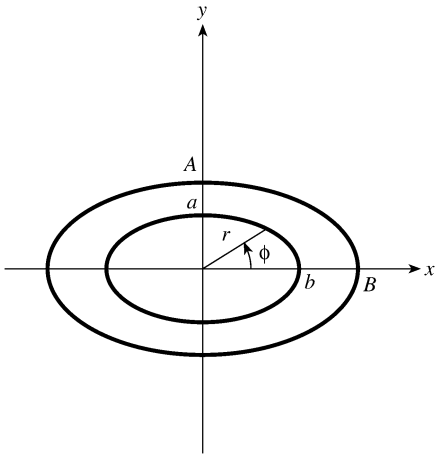

Figure 9.14
For Prob. 9.6.

the inner ellipse, for example,

$$r = \frac{a}{\sqrt{\sin^2 \phi + \nu^2 \cos^2 \phi}}, \qquad \nu = \frac{a}{b}$$

By modifying the MOL codes used in Example 9.3, plot the potential for $\phi = 0$, $a < \rho < b$.

© 2001 by CRC PRESS LLC

9.7 Solve Prob. 2.8 using MOL and compare your result with the exact solution

$$V(\rho, z) = \frac{4V_o}{\pi} \sum_{n=\text{odd}} \frac{I_0(n\pi\rho/L)}{nI_0(n\pi a/L)} \sin\left(\frac{n\pi z}{L}\right)$$

Take $L = 2a = 1$ m and $V_o = 10$ V.

9.8 Rework Example 9.4 for a pair of coupled microstrips shown in Fig. 9.15. Let $\epsilon_r = 10.2$, $w = 1.5$, $s/d = 1.5$, $a/d = 20$, $h/d = 19$, and $d = 1$ cm. Plot the effective dielectric constant versus d/λ_o.

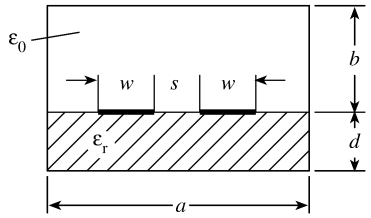

Figure 9.15
For Prob. 9.8.

9.9 Given the difference operator

$$[P] = \begin{bmatrix} 2 & -s^{*2} & \dots & & -s^2 \\ -s^2 & 2 & -s^{*2} & \dots & \\ & \ddots & \ddots & \ddots & \\ & & & & -s^{*2} \\ -s^{*2} & \dots & & -s^2 & 2 \end{bmatrix}$$

which is Hermitian, i.e., $[P] = [P^*]$. Show that $[P]$ has the following eigenvalues

$$\lambda_k^2 = 4\sin^2\frac{\phi_k \beta h}{2}\ ,\ \ \phi_k = \frac{2\pi k}{N}\ ,\ \ k = 1, 2, \dots, N$$

and the eigenvector matrices

$$T_{ik}^{(e)} = \frac{1}{\sqrt{N}} e^{ji\phi_k}\ , \quad T_{ik}^{(h)} = \frac{1}{\sqrt{N}} e^{j(i+0.5)\phi_k}$$

where $s = e^{j\beta h/2}$, s^* is the complex conjugate of s, β is the propagation constant, and h is the step size.

© 2001 by CRC PRESS LLC

9.10 Show that for

$$[P] = \begin{bmatrix} 2 & -1/s & \dots & & -s \\ -s & 2 & -1/s & \dots & \\ & \ddots & \ddots & \ddots & \\ & & & & -1/s \\ -1/s & \dots & & -s & 2 \end{bmatrix}$$

the eigenvalue matrices remain the same as in the previous problem.

© 2001 by CRC PRESS LLC